

Production and decay of hyperons in a transversely polarized electron-positron collider

Xu Cao,^{1,2,3,*} Yu-Tie Liang,^{1,2,†} and Rong-Gang Ping^{4,2,‡}

¹*Institute of Modern Physics, Chinese Academy of Sciences, Lanzhou 730000, China*

²*University of Chinese Academy of Sciences, Beijing 100049, China*

³*Research Center for Hadron and CSR Physics, Lanzhou University*

and Institute of Modern Physics of CAS, Lanzhou 730000, China

⁴*Institute of High Energy Physics, Chinese Academy of Sciences, Beijing 100049, China*

(Dated: July 16, 2024)

The self-polarization of relativistic electrons or positrons moving in a magnetic field at a storage ring occurs through the emission of spin-flip synchrotron radiation, known as the Sokolov-Ternov effect. The resulting transverse polarizations of the colliding electrons and positrons, away from the depolarization resonances, allow for precise investigation of the spin entangled hyperon-antihyperon pairs via virtual photon or charmonium decay. The feasibility study reveals a promising increase in the statistical sensitivity of the CP violation signal after considering the transverse polarizations of the lepton beams.

I. INTRODUCTION

Transversely-polarized beams at an electron-positron collider are particularly interesting in the search for new sources of CP violation through the measurement of CP odd azimuthal asymmetry [1]. They also offer a potential opportunity for revealing fundamental interactions and probing new physics [2]. For instance, some of specific modulations of azimuthal distributions would originate from the interference of operators of new physics beyond the Standard Model (SM) with those in the SM [3]. Additionally, transverse-polarization monitoring is a key technique for beam energy calibration using the resonant depolarization method, thereby improving the measurement of the mass and width of narrow resonances, such as the Z -boson and J/ψ [4].

The well-known Sokolov-Ternov effect [5] refers to the spin-flip processes through synchrotron radiation emission, which results in a natural build-up of transverse polarization through the competition between radiation self-polarization and spin diffusion [6, 7]. In the mid-1970s, the ACO storage ring at Orsay [8] and the improved VEPP-2M at the Budker Institute of Nuclear Physics (BINP) [9] both approached the theoretical limit of polarization levels, approximately $P_0 = 8/5\sqrt{3} \simeq 92.4\%$. At a beam energy of 3.7 GeV, SPEAR II found the equilibrium value of polarization to be about 0.76 [10]. The degree of transverse beam polarization at the CERN Large Electron Positron storage ring (LEP) was observed to be around 9.1% [11]. In the future, it is possible to polarize the beams up to 10% in a few hours at a designed energy of 45.6 GeV at the high-energy Circular Electron-Positron Collider (CEPC) [12]. The same

level of transverse polarization of the beams is expected in the Future Circular Collider (FCC-ee) [13]. As the first and only ring to provide longitudinal lepton spin polarization at high energy (27.5 GeV), the production of polarized electron and positron beams in HERA relied on the Sokolov-Ternov effect, where the spin rotators on either side of the interaction points converted the polarization of the beam from transverse to longitudinal, or vice versa. High luminosity at SuperKEKB prevents the use of the Sokolov-Ternov effect from accumulating or yielding longitudinal polarization [14].

The characteristic rise time for the Sokolov-Ternov polarization to build up from an unpolarized state is given by:

$$\tau_0 = \frac{8}{5\sqrt{3}} \frac{m_e^2 c^2 \rho^2 R}{e^2 \hbar \gamma^5}, \quad (1)$$

where the Lorentz factor is $\gamma = E_e/m_e$, leading to $\tau_0 = 2.8$ hours at $E_e = 2.0$ GeV, using an average radius $R = 38$ meters and an effective radius $\rho = 9.3$ meters for BEPCII (Beijing Electron-Positron Collider). The degree of transverse polarization $P_T = P_0(1 - e^{-t/\tau_0})$ reaches 0.28 after one hour of beam injection, and it increases with the rise of beam energy over the same duration of injection time at the same accelerator. The depolarization resonances from imperfections in the magnetic field occur at certain energies determined by gyromagnetic anomaly, leading into vanishing polarization of beams. The realistic situation is, of course, more complicated due to many other sources of depolarization resonances. However, the degree of transverse polarization of the beams at BEPCII and future super τ -charm facility (STCF) [15], away from the depolarization resonances, is expected to be of fair magnitude, resulting in a sizable impact on the angular distribution of final particles.

For a long time, spin asymmetries and correlations in hyperon-pair production in unpolarized electron-positron collisions have been proposed to measure simultaneously the electric-magnetic form factors and decay parameters

*Electronic address: caoxu@impcas.ac.cn

†Electronic address: liangyt@impcas.ac.cn

‡Electronic address: pingrg@mail.ihep.ac.cn

of hyperons and anti-hyperons [16–18]. This approach allows for the investigation of CP nonconservation parameters with high precision [19–21]. Recently, CP violation in hyperon decays at super-charm-tau factories with a longitudinally polarized electron beam has been investigated [22, 23], building upon earlier efforts [24–26]. However, the effects from transverse beam polarization were never taken into account in the analysis and simulation of the $e^+e^- \rightarrow B\bar{B}$ reactions, except for some earlier attempts on angular distributions [27–29]. In particular, the hyperon transverse polarization in $\psi(3686) \rightarrow \Lambda\bar{\Lambda}$ [30] and $\Sigma^+\bar{\Sigma}^-$ decays [31] is expected to be affected by the transverse polarization of the lepton beams, as is the case for $\psi(3770)$ [32]. The transverse polarization of double-strange baryons Ξ observed with unprecedented accuracy by the BESIII collaboration in $\psi(3686) \rightarrow \Xi^-\bar{\Xi}^+$ [33, 34], $\Xi^0\bar{\Xi}^0$ [35], $\Xi(1530)^-\bar{\Xi}(1530)^+$ and $\Xi(1530)^-\bar{\Xi}^+$ [36] also requires further scrutiny. The polarization of most strange baryons Ω in $\psi(3686) \rightarrow \Omega^-\bar{\Omega}^+$ [37] deserves more attention if enough events are accumulated. Additionally, data from different isospin channels would be helpful for understanding the hyperon electromagnetic form factors [38].

In Section II, we provide an analytical illustration of the effect of the transverse polarizations of the lepton beams on the production and decay of hyperons. The numerical outcome of moments analysis and statistical significance test is presented in Section III. Finally, we summarize the results to conclude the paper in Section IV.

II. PRODUCTION AND DECAY CHAINS OF HYPERONS

1. Spin Density Matrix

As a start, we consider the annihilation of a particle-antiparticle pair ($f\bar{f}$) to a virtual photon (γ^*) of energy squared s : $f(\lambda_1)\bar{f}(\lambda_2) \rightarrow \gamma^*(\lambda)$. In this process, annihilation conserves helicity, yielding $\lambda = \lambda_1 - \lambda_2$. If the particle and antiparticle, both with mass M , are of the same spin 1/2, there are three helicity configurations: $(\lambda_1, \lambda_2) = (\pm 1/2, \pm 1/2), (-1/2, 1/2)$ and $(1/2, -1/2)$. There are four helicity amplitudes A_{λ_1, λ_2} , but only two are independent, for example, $A_{1/2, 1/2} = A_{-1/2, -1/2} = 2\sqrt{2}MG_E$ and $A_{1/2, -1/2} = A_{-1/2, 1/2} = 2\sqrt{s}G_M$. Here, $G_{E, M}$ are the electromagnetic form factors of the particle. If the particle (antiparticle) is the structureless electron (positron), the helicity of the electron and positron must be opposite; otherwise, the helicity amplitude with a vanishing helicity difference $\lambda_z = 0$ is suppressed by a factor of m_e/\sqrt{s} . As a result, the photon only couples right-handed particles to left-handed antiparticles and vice versa.

Due to synchrotron radiation when positrons and electrons circulate in the storage ring, the transition probabilities of the two spin projections of positrons and

electrons, guided by the magnetic field in the storage ring, are different. This causes the spin orientation of positrons to tend toward the direction of the guiding magnetic field, while the orientation of electrons is opposite. Consequently, as the lepton beam remains in the storage ring for an extended period, they will acquire a transverse polarization $\mathcal{P}_t = p_x + ip_y = P_T e^{i\phi_+}$ and $\bar{\mathcal{P}}_t = \bar{p}_x + i\bar{p}_y = \bar{P}_T e^{i\phi_-}$ for positron and electron, respectively, where $P_T = |\mathcal{P}_t|$. Here, $p_x(\bar{p}_x)$ represents the degree of transverse polarization in the scattering plane, and $p_y(\bar{p}_y)$ represents the degree of polarization perpendicular to the scattering plane [2]. The angles ϕ_+ and ϕ_- represent the azimuthal angles of the positron and electron polarizations, respectively, with respect to the lab system. In a positron-electron annihilation experiment with symmetric beam energy, the Sokolov–Ternov effect requires the equal degree of polarization $P_T = \bar{P}_T$ and $\phi_+ = \phi_- = \pi/2$. This means that the positron and the electron have the same polarization vector in the individual helicity frame¹. The spin density matrix of the leptons is represented in their helicity frame as:

$$\rho^- = \frac{1}{2} \begin{pmatrix} 1 + \mathcal{P}_z & \mathcal{P}_t \\ \mathcal{P}_t^* & 1 - \mathcal{P}_z \end{pmatrix} \text{ for } e^-,$$

$$\rho^+ = \frac{1}{2} \begin{pmatrix} 1 + \bar{\mathcal{P}}_z & \mathcal{P}_t \\ \mathcal{P}_t^* & 1 - \bar{\mathcal{P}}_z \end{pmatrix} \text{ for } e^+,$$

in the most general case of considering both a longitudinal and a transverse component of polarization vectors.

In the laboratory system, for the process of $e^+e^- \rightarrow \gamma^*/\psi$ annihilation, the spin density matrix (SDM) element of γ^*/ψ is given by:

$$\rho_{m, m'}^{\gamma^*/\psi} = \sum_{\lambda_1, \lambda'_1, \lambda_2, \lambda'_2} D_{m, \lambda_1 - \lambda_2}^{1*} (0, 0, 0) D_{m', \lambda'_1 - \lambda'_2}^1 (0, 0, 0) \times \rho_{\lambda_1, \lambda'_1}^+ \rho_{\lambda_2, \lambda'_2}^- \delta_{\lambda_1, -\lambda_2} \delta_{\lambda'_1, -\lambda'_2}, \quad (2)$$

where $\lambda_1, \lambda'_1(\lambda_2, \lambda'_2)$ represent the helicity values of positron (electron). The Dirac δ -function in the above equation ensures the conservation of helicity during the positron-electron annihilation process as discussed from the beginning of this subsection. Performing a simple algebraic calculation on the above equation, we obtain:

$$\rho^{\gamma^*/\psi} = \frac{1}{2} \begin{pmatrix} (1 - \mathcal{P}_z)(1 + \bar{\mathcal{P}}_z) & 0 & P_T^2 \\ 0 & 0 & 0 \\ P_T^2 & 0 & (1 - \mathcal{P}_z)(1 + \bar{\mathcal{P}}_z) \end{pmatrix},$$

Based on the spin density matrix, we conduct a simple analysis of the polarization of γ^*/ψ . For a particle with

¹ In an e^+e^- storage ring, the z -axes of the helicity frames for the electron and positron are aligned with their respective directions of motion, and they share the same x -axis along the radical direction, while the vertical y -axis is oriented in the opposite direction.

spin $s = 1$, its overall degree of polarization is defined by $d = \frac{1}{\sqrt{2s}}[(2s+1)\text{Tr}(\rho^{\psi^2}) - 1]^{1/2} = \sqrt{1 + 3\mathcal{P}_z^2 + 3P_T^4}/2$ by taking $\mathcal{P}_z = 0$ for simplicity, indicating that the presence of P_T increases the overall degree of polarization of γ^*/ψ state as well as the \mathcal{P}_z . This polarization has two sources:

$$\rho^{\gamma^*/\psi} = \frac{1}{3} \begin{pmatrix} 1 + \frac{3q_z}{2} + \sqrt{\frac{3}{2}}(T_{xx} + T_{yy} + 2T_{zz}) & \frac{3(q_x - iq_y)}{2\sqrt{2}} & \sqrt{\frac{3}{2}}(T_{xx} - T_{yy}) \\ \frac{3(q_x + iq_y)}{2\sqrt{2}} & 1 + \sqrt{6}T_{xx} + \sqrt{6}T_{yy} & \frac{3(q_x - iq_y)}{2\sqrt{2}} \\ \sqrt{\frac{3}{2}}(T_{xx} - T_{yy}) & \frac{3(q_x + iq_y)}{2\sqrt{2}} & 1 - \frac{3q_z}{2} + \sqrt{\frac{3}{2}}(T_{xx} + T_{yy} + 2T_{zz}) \end{pmatrix}. \quad (3)$$

Comparing the elements of the ρ^{ψ} matrix, we can obtain $q_x = q_y = 0$, $q_z = -\mathcal{P}_z$, $T_{xx} = \frac{3P_T^2 - 1}{2\sqrt{6}}$, $T_{yy} = -\frac{1+3P_T^2}{2\sqrt{6}}$, $T_{zz} = 1/\sqrt{6}$ with other $T_{ij}(i \neq j) = 0$. It can be seen that the tensor polarization of $\rho^{\gamma^*/\psi}$ comes from the spin correlation and transverse polarization of the initial lepton beams, with linear polarization being solely from the longitudinal polarization of beams. In the following paper, we focus solely on the transverse polarization of the initial lepton beams. The study of a longitudinally polarized electron beam has been recently addressed independently in other studies [22, 23].

$$2. \quad e^+e^- \rightarrow \gamma^*/\psi \rightarrow \Lambda(p\pi^-)\bar{\Lambda}(\bar{p}\pi^+)$$

In the laboratory system, the decayed Λ particle moves in the direction defined by polar and azimuthal angles (θ, ϕ) . We calculate the joint angular distribution in the Λ helicity system, as illustrated in Fig. 1. In this system, the z -axis aligns with the Λ particle's direction of motion, the y -axis is perpendicular to the Λ production plane, i.e., $\hat{y} = \hat{p}_+ \times \hat{p}_\Lambda$, where \hat{p}_+ and \hat{p}_Λ are the unit momentum vectors for the positron and Λ , respectively. The x -axis lies in the Λ production plane, forming a right-handed x - y - z coordinate system. After boosting the momenta of p and π^- in laboratory frame to the Λ rest frame, they define the Λ decay plane together with the momenta of Λ in laboratory frame. The angle between the proton momen-

one is the linear polarization $\mathcal{Q} = (q_x, q_y, q_z)$, and the other is the tensor polarization $T_{ij}(i, j = x, y, z)$. The spin density matrix elements of ρ^{ψ} can be expressed using \mathcal{Q} and T_{ij}

tum in the Λ decay plane and Λ momentum in laboratory frame is defined as θ_1 , and the angle between the Λ production and decay plane is defined as ϕ_1 . Similar helicity angles (θ_2, ϕ_2) are defined in the same manner. In the Λ helicity system, the J/ψ SDM is calculated by transforming it from the laboratory system to this helicity system, as follows:

$$\begin{aligned} \rho_1^{i,j}(\theta, \phi) &\equiv \sum_{k,k'=\pm 1} \rho_{k,k'}^{\gamma^*/\psi} \mathcal{D}_{k,i}^{1*}(\phi, \theta, 0) \mathcal{D}_{k',j}^1(\phi, \theta, 0) \\ &= \sum_{k=\pm 1} [\mathcal{D}_{k,i}^{1*}(\phi, \theta, 0) \mathcal{D}_{k,j}^1(\phi, \theta, 0) \\ &\quad + P_T^2 \mathcal{D}_{k,i}^{1*}(\phi, \theta, 0) \mathcal{D}_{-k,j}^1(\phi, \theta, 0)]. \end{aligned} \quad (4)$$

Thus the effects from transverse beam polarization occur only if both beams are polarized and generate interference terms between left- and right-helicity amplitudes [29]. The explicit form of the reduced ρ_1 is given by

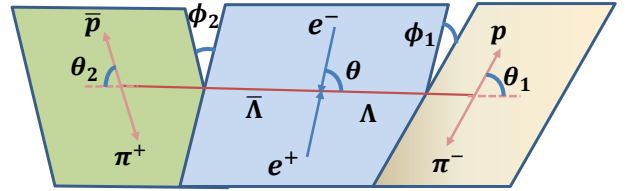


FIG. 1: Helicity frame defined for the $\psi \rightarrow \Lambda(p\pi^-)\bar{\Lambda}(\bar{p}\pi^+)$.

$$\begin{aligned} \rho_1(\theta, \phi) &= \frac{1}{2} \cdot \begin{pmatrix} \frac{1+\cos^2\theta}{2} & -\frac{\cos\theta\sin\theta}{\sqrt{2}} & \frac{\sin^2\theta}{2} \\ -\frac{\cos\theta\sin\theta}{\sqrt{2}} & \sin^2\theta & \frac{\cos\theta\sin\theta}{\sqrt{2}} \\ \frac{\sin^2\theta}{2} & \frac{\cos\theta\sin\theta}{\sqrt{2}} & \frac{1+\cos^2\theta}{2} \end{pmatrix} \\ &+ \frac{1}{2} P_T^2 \cdot \begin{pmatrix} \frac{\sin^2\theta}{2} \cos 2\phi & \frac{\cos\theta\sin\theta}{\sqrt{2}} \cos 2\phi - i \frac{\sin\theta}{\sqrt{2}} \sin 2\phi & \frac{1+\cos^2\theta}{2} \cos 2\phi - i \cos\theta \sin 2\phi \\ \frac{\cos\theta\sin\theta}{\sqrt{2}} \cos 2\phi + i \frac{\sin\theta}{\sqrt{2}} \sin 2\phi & -\sin^2\theta \cos 2\phi & -\frac{\cos\theta\sin\theta}{\sqrt{2}} \cos 2\phi + i \frac{\sin\theta}{\sqrt{2}} \sin 2\phi \\ \frac{1+\cos^2\theta}{2} \cos 2\phi + i \cos\theta \sin 2\phi & -\frac{\cos\theta\sin\theta}{\sqrt{2}} \cos 2\phi - i \frac{\sin\theta}{\sqrt{2}} \sin 2\phi & \frac{\sin^2\theta}{2} \cos 2\phi \end{pmatrix}. \end{aligned} \quad (5)$$

The density matrix for the production process is the sum of the contributions from the two helicities [22, 39]:

$$\rho_{B\bar{B}}^{\lambda_1, \lambda_2; \lambda'_1, \lambda'_2} \propto A_{\lambda_1, \lambda_2} A_{\lambda'_1, \lambda'_2}^* \rho_1^{\lambda_1 - \lambda_2, \lambda'_1 - \lambda'_2}, \quad (6)$$

with the helicity amplitudes of the photon transition to a pair of baryon-antibaryon $A_{1/2, 1/2} = A_{-1/2, -1/2} = \sqrt{(1 - \alpha_\psi)/2}$ and $A_{1/2, -1/2} = A_{-1/2, 1/2} = \sqrt{1 + \alpha_\psi} e^{-i\Delta\Phi}$. Here $\alpha_\psi = (M_\psi^2 |G_M^\psi|^2 - 4M_B^2 |G_E^\psi|^2) / (M_\psi^2 |G_M^\psi|^2 + 4M_B^2 |G_E^\psi|^2)$ is the decay parameter of charmonium to baryon-antibaryon, and the $\Delta\Phi = \arg(G_E^\psi / G_M^\psi)$ is the relative phase between ψ electric and magnetic form factors.

The general expression for the joint density matrix of the $B\bar{B}$ pair is:

$$\rho_{B\bar{B}} = \sum_{\mu, \nu=0}^3 C_{\mu\nu} \sigma_\mu^B \otimes \sigma_\nu^{\bar{B}}, \quad (7)$$

where a set of four Pauli matrices $\sigma_\mu^B (\sigma_\nu^{\bar{B}})$ in the $B(\bar{B})$ rest frame is used and $C_{\mu\nu} = C_{\mu\nu}^U + C_{\mu\nu}^T$ is a 4×4 real matrix representing polarizations and spin correlations of the baryons. The elements of the $C_{\mu\nu}$ matrix are functions of the production angle $\Omega(\theta, \phi)$ of the B baryon:

$$(C_{\mu\nu}) = \frac{3}{3 + \alpha_\psi} \cdot \begin{pmatrix} 1 + \alpha_\psi \cos^2\theta & 0 & \beta_\psi \sin\theta \cos\theta & 0 \\ 0 & \sin^2\theta & 0 & \gamma_\psi \sin\theta \cos\theta \\ -\beta_\psi \sin\theta \cos\theta & 0 & \alpha_\psi \sin^2\theta & 0 \\ 0 & -\gamma_\psi \sin\theta \cos\theta & 0 & -\alpha_\psi - \cos^2\theta \end{pmatrix} + \frac{3P_T^2}{3 + \alpha_\psi} \cdot \begin{pmatrix} \alpha_\psi \sin^2\theta \cos 2\phi & -\beta_\psi \sin\theta \sin 2\phi & -\beta_\psi \sin\theta \cos\theta \cos 2\phi & 0 \\ -\beta_\psi \sin\theta \sin 2\phi & (\alpha_\psi + \cos^2\theta) \cos 2\phi & -(1 + \alpha_\psi) \cos\theta \sin 2\phi & -\gamma_\psi \sin\theta \cos\theta \cos 2\phi \\ \beta_\psi \sin\theta \cos\theta \cos 2\phi & (1 + \alpha_\psi) \cos\theta \sin 2\phi & (1 + \alpha_\psi \cos^2\theta) \cos 2\phi & -\gamma_\psi \sin\theta \sin 2\phi \\ 0 & \gamma_\psi \sin\theta \cos\theta \cos 2\phi & -\gamma_\psi \sin\theta \sin 2\phi & -\sin^2\theta \cos 2\phi \end{pmatrix}, \quad (8)$$

with $\beta_\psi = \sqrt{1 - \alpha_\psi^2} \sin\Delta\Phi$ and $\gamma_\psi = \sqrt{1 - \alpha_\psi^2} \cos\Delta\Phi$.

Therefore a transverse polarization of the final state baryon is only allowed in the direction normal to the plane spanned by the incoming beam and the outgoing baryon:

$$P_y^B = \frac{\beta_\psi \sin\theta \cos\theta (1 - P_T^2 \cos 2\phi)}{1 + \alpha_\psi \cos^2\theta + \alpha_\psi P_T^2 \sin^2\theta \cos 2\phi}, \quad (9)$$

$$P_x^B = \frac{-P_T^2 \beta_\psi \sin\theta \sin 2\phi}{1 + \alpha_\psi \cos^2\theta + \alpha_\psi P_T^2 \sin^2\theta \cos 2\phi}, \quad (10)$$

with vanishing longitudinal polarization component. Besides, the transverse polarization of beams introduces two new correlations $C_{xy} = -C_{yx}$, $C_{yz} = C_{zy}$ in addition to the four existing ones, which further constrain the decay parameters of hyperons, and thus provides more stringent tests of the CP violation.

The baryon angular distribution is

$$\frac{4\pi}{\sigma} \frac{d\sigma}{d\Omega_B} = \frac{3}{3 + \alpha_\psi} (1 + \alpha_\psi \cos^2\theta + \alpha_\psi P_T^2 \sin^2\theta \cos 2\phi) \quad (11)$$

and Fig. 2 shows its three dimensional distribution. So that if the transverse polarization of the final-state particles is not measured, the effects of transverse polarizations are absent in the ϕ -averaged cross section, albeit,

present in the θ -averaged cross section:

$$\frac{2\pi}{\sigma} \frac{d\sigma}{d\phi} = -2 \cos\theta_0 \frac{3 + \alpha_\psi \cos^2\theta_0 + \alpha_\psi P_T^2 \cos 2\phi (3 - \cos^2\theta_0)}{3 + \alpha_\psi}, \quad (12)$$

with $(\theta_0, \pi - \theta_0)$ being the detector coverage of the solid angle around the interaction point (IP). Therefore the degree of transverse polarization would be measured through $e^+e^- \rightarrow \mu^+\mu^-$ and e^+e^- azimuth angular distributions. The distribution of scattering angle has been previously explored in BES [40], BESIII [41] and KEDR at the VEPP-4M [42], but the azimuth distributions did not receive any attention.

There are five global parameters to describe a process $e^+e^- \rightarrow B\bar{B}$ followed by single-step weak two-body decays of the hyperon B and the antihyperon \bar{B} [39]. For decay $B \rightarrow b\pi$ and the corresponding charge conjugate (c.c.) decay mode $\bar{B} \rightarrow \bar{b}\pi$, like $e^+e^- \rightarrow \gamma^*/\psi \rightarrow \Lambda(p\pi^-)\bar{\Lambda}(\bar{p}\pi^+)$, they are represented by the vector $\boldsymbol{\omega} \equiv (\alpha_\psi, \Delta\Phi, \alpha_-, \alpha_+)$ with *a priori* known P_T^2 and α_- (or α_+) being the decay parameter of $B \rightarrow b\pi$ (or $\bar{B} \rightarrow \bar{b}\pi$). The joint angular distribution $\mathcal{W}(\boldsymbol{\xi})$ can be expressed with respect to the vector $\boldsymbol{\xi} \equiv (\Omega_B, \Omega_b, \Omega_{\bar{b}})$ representing a complete set of the kinematic variables describing a single-event configuration in the six dimensional phase space [23, 43]:

$$\mathcal{W}(\boldsymbol{\xi}) = \mathcal{F}_0 + \beta_\psi (\alpha_+ \mathcal{F}_3 - \alpha_- \mathcal{F}_4) + \alpha_- \alpha_+ (\mathcal{F}_1 + \gamma_\psi \mathcal{F}_2 + \alpha_\psi \mathcal{F}_5), \quad (13)$$

where the angular function $\mathcal{F}_i(\xi)$ ($i = 0, 1, \dots, 5$) are defined as

$$\begin{aligned}
\mathcal{F}_0 &= 1 + \alpha_\psi \cos^2 \theta + \alpha_\psi P_T^2 \sin^2 \theta \cos 2\phi, \\
\mathcal{F}_1 &= (\sin^2 \theta + P_T^2 \cos 2\phi \cos^2 \theta) \sin \theta_1 \cos \phi_1 \sin \theta_2 \cos \phi_2 \\
&\quad - (\cos^2 \theta + P_T^2 \cos 2\phi \sin^2 \theta) \cos \theta_1 \cos \theta_2 \\
&\quad + P_T^2 \sin \theta_1 \sin \theta_2 (\sin 2\phi \cos \theta \sin(\phi_1 - \phi_2) + \cos 2\phi \sin \phi_1 \sin \phi_2), \\
\mathcal{F}_2 &= (1 - P_T^2 \cos 2\phi) \sin \theta \cos \theta (\sin \theta_1 \cos \theta_2 \cos \phi_1 - \cos \theta_1 \sin \theta_2 \cos \phi_2) \\
&\quad - P_T^2 \sin 2\phi \sin \theta (\sin \theta_1 \cos \theta_2 \sin \phi_1 + \cos \theta_1 \sin \theta_2 \sin \phi_2), \\
\mathcal{F}_3 &= (1 - P_T^2 \cos 2\phi) \sin \theta \cos \theta \sin \theta_2 \sin \phi_2 - P_T^2 \sin 2\phi \sin \theta \sin \theta_2 \cos \phi_2, \\
\mathcal{F}_4 &= (1 - P_T^2 \cos 2\phi) \sin \theta \cos \theta \sin \theta_1 \sin \phi_1 + P_T^2 \sin 2\phi \sin \theta \sin \theta_1 \cos \phi_1, \\
\mathcal{F}_5 &= (\sin^2 \theta + P_T^2 \cos 2\phi \cos^2 \theta) \sin \theta_1 \sin \phi_1 \sin \theta_2 \sin \phi_2 - \cos \theta_1 \cos \theta_2 \\
&\quad + P_T^2 \sin \theta_1 \sin \theta_2 [\sin 2\phi \cos \theta \sin(\phi_1 - \phi_2) + \cos 2\phi \cos \phi_1 \cos \phi_2],
\end{aligned} \tag{14}$$

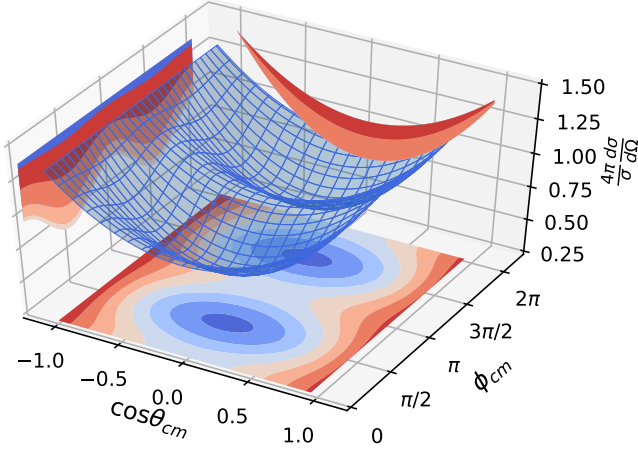


FIG. 2: The three dimensional plot and the projection of angular distribution of Λ hyperon in $e^+e^- \rightarrow \psi(3686) \rightarrow \Lambda\bar{\Lambda}$ with $\alpha = 0.69$ and $\Delta\Phi = 23^\circ$ [30], and $P_T = 0.5$.

where the $\Omega_b(\theta_1, \phi_1)$ (or $\Omega_{\bar{b}}(\theta_2, \phi_2)$) are the spherical coordinates of b (or \bar{b}) relative to B (or \bar{B}) in the helicity frame of B (or \bar{B}). The *helicity angles* are used here to parameterize the multidimensional phase space, which are in following the angular convention with those previous works [22, 23].

One can always define corresponding asymmetries in terms of events to select the $\cos 2\phi$ modulation as

$$\mathcal{W}_{\cos 2\phi}^+(\xi) = \int_0^{\pi/4} + \int_{3\pi/4}^{5\pi/4} + \int_{7\pi/4}^{2\pi} \mathcal{W}(\xi) d\phi, \tag{15}$$

$$\mathcal{W}_{\cos 2\phi}^-(\xi) = \int_{\pi/4}^{3\pi/4} + \int_{5\pi/4}^{7\pi/4} \mathcal{W}(\xi) d\phi, \tag{16}$$

the latter of which is corresponding to the number of events in the range of upper semi-sphere 45° to 135° and

225° to 315° , and the former is the number of events in the remaining lower semi-sphere. Then $\mathcal{W}^+(\xi) - \mathcal{W}^-(\xi)$ is proportional to those terms of $P_T^2 \cos 2\phi$ dependence and $\mathcal{W}^+(\xi) + \mathcal{W}^-(\xi)$ integrates out the P_T^2 terms which are of $\cos 2\phi$ modulation. To select the $\sin 2\phi$ modulation:

$$\mathcal{W}_{\sin 2\phi}^+(\xi) = \int_0^{\pi/2} + \int_{\pi}^{3\pi/2} \mathcal{W}(\xi) d\phi, \tag{17}$$

$$\mathcal{W}_{\sin 2\phi}^-(\xi) = \int_{\pi/2}^{\pi} + \int_{3\pi/2}^{2\pi} \mathcal{W}(\xi) d\phi, \tag{18}$$

the former of which is corresponding to the number of events in the range of upper semi-sphere 0° to 90° and 180° to 270° , and the latter is the number of events in the remaining lower semi-sphere. Fig. 3 shows the transverse polarization P_y and P_x of baryon in all azimuthal angles in comparison of upper and lower spheres. Instead, one can investigate the moments of the joint angular distributions as shown in Sec. III.

If identifying the decay chain of the hyperon with summation over the antihyperon spin directions, so called single tag events:

$$\mathcal{W}(\xi) = \mathcal{F}_0 - \beta_\psi \alpha_- \mathcal{F}_4, \tag{19}$$

which is useful to increase the statistical events if the transverse polarization of beams is of small degree.

$$3. \quad e^+e^- \rightarrow \gamma^*/\psi \rightarrow \Xi^-(\Lambda\pi^-)\Xi^+(\bar{\Lambda}\pi^+)$$

The definition of the helicity system for the first two decays in the processes $e^+e^- \rightarrow \gamma^*/\psi \rightarrow \Xi^-\Xi^+$ with $\Xi \rightarrow \Lambda\pi$ and $\bar{\Xi} \rightarrow \bar{\Lambda}\pi^+$ is similar to that of $e^+e^- \rightarrow \psi \rightarrow \Lambda(p\pi^-)\bar{\Lambda}(\bar{p}\pi^+)$, as shown in Fig. 4. For the subsequent decays of $\Lambda(\bar{\Lambda}) \rightarrow p\pi^-(\bar{p}\pi^+)$, the polar angle $\theta_3(\theta_4)$

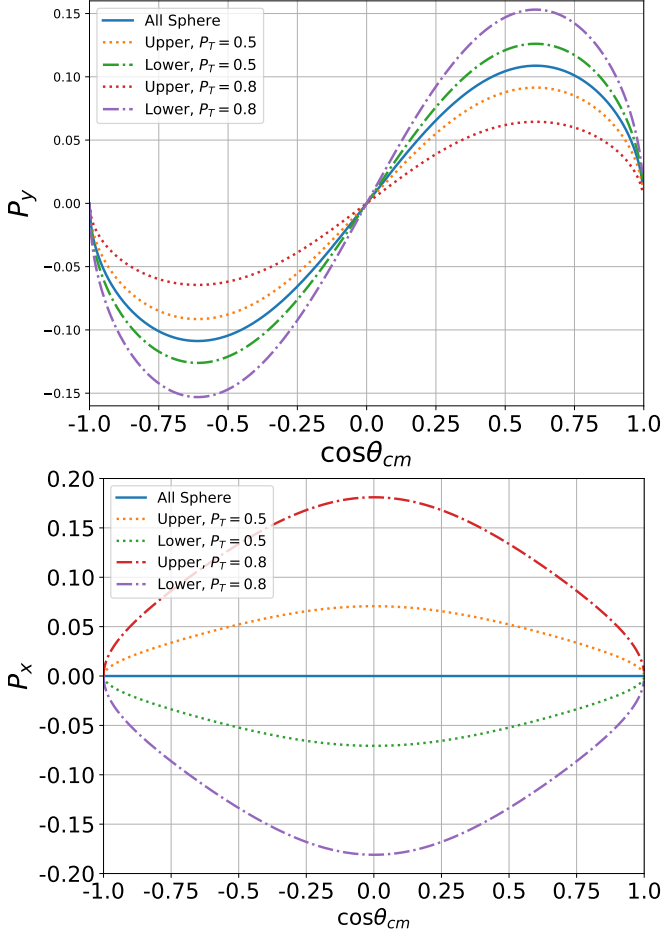


FIG. 3: The transverse polarization P_y and P_x of Λ hyperon in all azimuthal angles in comparison of upper and lower spheres. The parameters of $e^+e^- \rightarrow \psi(3686) \rightarrow \Lambda\bar{\Lambda}$ with $\alpha_\psi = 0.69$ and $\Delta\Phi = 23^\circ$ [30] are used.

is defined as the angle between the momentum of the proton (anti-proton) and $\Lambda(\bar{\Lambda})$ in the respective mother rest frame, and the azimuthal angle $\phi_3(\phi_4)$ is defined as the angle between the $\Lambda(\bar{\Lambda})$ production and decay plane.

$$(D_{\Xi}^\mu) = \begin{pmatrix} 1 + \alpha_1\alpha_3 \cos\theta_3 \\ \alpha_1 \sin\theta_1 \cos\phi_1 + \alpha_3 [\sin\theta_1 \cos\phi_1 \cos\theta_3 - \sin\phi_1 \sin\theta_3 (\beta_1 \cos\phi_3 + \gamma_1 \sin\phi_3) + \cos\theta_1 \cos\phi_1 \sin\theta_3 (\gamma_1 \cos\phi_3 - \beta_1 \sin\phi_3)] \\ \alpha_1 \sin\theta_1 \sin\phi_1 + \alpha_3 [\sin\theta_1 \sin\phi_1 \cos\theta_3 + \cos\phi_1 \sin\theta_3 (\beta_1 \cos\phi_3 + \gamma_1 \sin\phi_3) + \cos\theta_1 \sin\phi_1 \sin\theta_3 (\gamma_1 \cos\phi_3 - \beta_1 \sin\phi_3)] \\ \alpha_1 \cos\theta_1 + \alpha_3 [\cos\theta_1 \cos\theta_3 - \sin\theta_1 \sin\theta_3 (\gamma_1 \cos\phi_3 - \beta_1 \sin\phi_3)] \end{pmatrix},$$

with the substitution of $\{1, 3\} \rightarrow \{2, 4\}$ for \bar{D}_{Ξ}^ν . This joint angular distribution, without explicit consideration of transverse polarization of beams, has been previously calculated in the literature. [43, 44]. For simplicity we demonstrate

The vector $\xi := (\theta, \phi, \theta_1, \phi_1, \theta_2, \phi_2, \theta_3, \phi_3, \theta_4, \phi_4)$ represents a complete set of the kinematic variables describing a single-event configuration in the ten-dimensional phase space, in line with the above definition of spherical coordinates in the helicity systems.

There are six global parameters to describe the complete angular distribution, represented by the vector $\omega \equiv (\alpha_\psi, \Delta\Phi, \alpha_1, \bar{\alpha}_2, \alpha_3, \bar{\alpha}_4)$. The joint angular distribution reads:

$$\begin{aligned} \mathcal{W}(\xi) = & \mathcal{D}_{\Xi}^0 \bar{\mathcal{D}}_{\Xi}^0 C_{00} + \mathcal{D}_{\Xi}^1 \bar{\mathcal{D}}_{\Xi}^1 C_{xx} + \mathcal{D}_{\Xi}^2 \bar{\mathcal{D}}_{\Xi}^2 C_{yy} + \mathcal{D}_{\Xi}^3 \bar{\mathcal{D}}_{\Xi}^3 C_{zz} \\ & + (\mathcal{D}_{\Xi}^1 \bar{\mathcal{D}}_{\Xi}^2 - \mathcal{D}_{\Xi}^2 \bar{\mathcal{D}}_{\Xi}^1) C_{xy} + (\mathcal{D}_{\Xi}^1 \bar{\mathcal{D}}_{\Xi}^3 - \mathcal{D}_{\Xi}^3 \bar{\mathcal{D}}_{\Xi}^1) C_{xz} \\ & + (\mathcal{D}_{\Xi}^2 \bar{\mathcal{D}}_{\Xi}^3 + \mathcal{D}_{\Xi}^3 \bar{\mathcal{D}}_{\Xi}^2) C_{yz} + (\mathcal{D}_{\Xi}^0 \bar{\mathcal{D}}_{\Xi}^1 + \mathcal{D}_{\Xi}^1 \bar{\mathcal{D}}_{\Xi}^0) P_x \\ & + (\mathcal{D}_{\Xi}^0 \bar{\mathcal{D}}_{\Xi}^2 - \mathcal{D}_{\Xi}^2 \bar{\mathcal{D}}_{\Xi}^0) P_y, \end{aligned} \quad (20)$$

with vanishing P_z here. The parameters C_{ij} and P_i ($i = 0$ or x, y, z) are given in Eq. (8) with the substitution of α_ψ and $\Delta\Phi$ for those of $\gamma^*/\psi \rightarrow \Xi^- \bar{\Xi}^+$, and $\mathcal{D}_{\Xi}^\mu(\Omega_{\Xi}(\theta_1, \phi_1), \Omega_{\Lambda}(\theta_3, \phi_3))$ is the decay matrix of $\Xi \rightarrow \Lambda\pi$, $\bar{\Lambda} \rightarrow \bar{p}\pi^-$, and $\bar{\mathcal{D}}_{\Xi}^\nu(\Omega_{\Xi}(\theta_2, \phi_2), \Omega_{\bar{\Lambda}}(\theta_4, \phi_4))$ is for $\bar{\Xi} \rightarrow \bar{\Lambda}\pi$, $\bar{\Lambda} \rightarrow \bar{p}\pi^-$, respectively. The \mathcal{D}_{Ξ}^μ matrix elements are explicitly written as [39]:

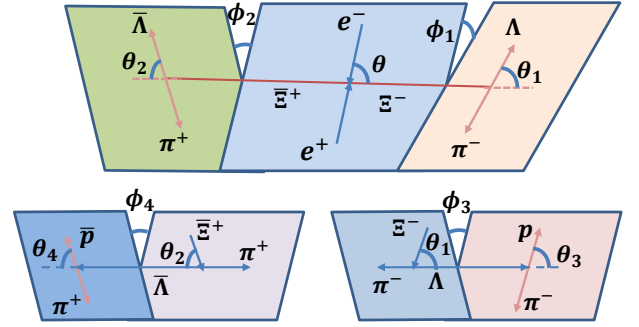


FIG. 4: Upper panel: Helicity frame defined for the $\psi \rightarrow \Xi^-(\Lambda\pi^-)\bar{\Xi}^+(\bar{\Lambda}\pi^+)$. Lower panel: Helicity frame defined for $\Lambda(\bar{\Lambda}) \rightarrow p\pi^-(\bar{p}\pi^+)$.

those joint angular distributions of single tag events with summation over the Ξ antihyperon spin directions:

$$\begin{aligned} \mathcal{W}(\xi) = & (1 + \alpha_\psi \cos^2 \theta + \alpha_\psi P_T^2 \sin^2 \theta \cos 2\phi)(1 + \alpha_\Xi \alpha_\Lambda \cos \theta_3) \\ & - P_T^2 \sin 2\phi \beta_\psi \sin \theta \{ \alpha_\Xi \sin \theta_1 \cos \phi_1 \\ & + \alpha_\Lambda [\sin \theta_1 \cos \phi_1 \cos \theta_3 - \sin \phi_1 \sin \theta_3 (\beta_\Xi \cos \phi_3 + \gamma_\Xi \sin \phi_3) + \cos \theta_1 \cos \phi_1 \sin \theta_3 (\gamma_\Xi \cos \phi_3 - \beta_\Xi \sin \phi_3)] \} \\ & - (1 - P_T^2 \cos 2\phi) \beta_\psi \sin \theta \cos \theta \{ \alpha_\Xi \sin \theta_1 \sin \phi_1 \\ & + \alpha_\Lambda [\sin \theta_1 \sin \phi_1 \cos \theta_3 + \cos \phi_1 \sin \theta_3 (\beta_\Xi \cos \phi_3 + \gamma_\Xi \sin \phi_3) + \cos \theta_1 \sin \phi_1 \sin \theta_3 (\gamma_\Xi \cos \phi_3 - \beta_\Xi \sin \phi_3)] \}, \end{aligned} \quad (21)$$

After integrating out the P_T terms [44, 45] it is used in the measurement of Λ_c case [46].

III. DISCUSSIONS

At the unpolarized electron-positron collider, the parasitic production of transverse polarization of beams provides new degrees of freedom for physical research. Compared to the unpolarized beams, the formulas describing particle production and decay become more complex, but on the other hand, they provide us with more observational degrees of freedom to study the dynamics of decay processes. The transverse polarization effect, in addition to being prominently expressed in the angular distribution of final-state particles, can also be manifested in the moment distribution of particles at various decay levels. Furthermore, the presence of transverse polarization provides additional polarization information for measuring the asymmetry parameters of hyperon decay, which is beneficial for improving measurement accuracy, for instance, the CP violation parameters as shown in the following analysis.

A. Moments analysis

For instance, we construct the following observables by using the angles $\theta_1, \theta_2, \phi_1$, and ϕ_2 detected in the process of $e^+e^- \rightarrow \psi(3686) \rightarrow \Lambda\bar{\Lambda}, \Lambda \rightarrow p\pi^-, \bar{\Lambda} \rightarrow \bar{p}\pi^+$,

$$\begin{aligned} \mu_1 &= \sin \theta_1 \sin \theta_2 [\sin(2\phi) \cos \theta \sin(\phi_1 - \phi_2) \\ &+ \cos(2\phi) \sin \phi_1 \sin \phi_2], \\ \mu_2 &= \cos(2\phi) \sin \theta \cos \theta [\sin \theta_1 \cos \theta_2 \cos \phi_1 \\ &- \cos \theta_1 \sin \theta_2 \cos \phi_2], \\ \mu_3 &= \sin(2\phi) \sin \theta \cos \phi_2, \\ \mu_4 &= \sin(2\phi) \sin \theta \cos \phi_1, \\ \mu_5 &= \sin \theta_1 \sin \theta_2 [\sin(2\phi) \cos \theta \sin(\phi_1 - \phi_2) \\ &- \cos(2\phi) \cos \phi_1 \cos \phi_2]. \end{aligned} \quad (22)$$

The moments derived from these observables represent taking their averages over the joint angular distribution. Their moments with respect to the $\cos \theta$ angular distribution

are expressed as:

$$\frac{d\langle \mu_i \rangle}{d \cos \theta} = \frac{\int \mathcal{W}(\xi) \mu_i d \cos \theta_1 d \cos \theta_2 d \phi_1 d \phi_2}{\int \mathcal{W}(\xi) d \cos \theta_1 d \cos \theta_2 d \phi_1 d \phi_2}, \quad (i = 1, 2, \dots, 5). \quad (23)$$

Then one has

$$\begin{aligned} \frac{d\langle \mu_1 \rangle}{d \cos \theta} &= \frac{\alpha_- \alpha_+ P_T^2 [(3\alpha_\psi + 2) \cos^2 \theta + 1]}{12(\alpha_\psi + 3)}, \\ \frac{d\langle \mu_2 \rangle}{d \cos \theta} &= -\frac{\alpha_- \alpha_+ P_T^2 \gamma_\psi \sin^2 \theta \cos^2 \theta}{6(\alpha_\psi + 3)}, \\ \frac{d\langle \mu_3 \rangle}{d \cos \theta} &= -\frac{3\alpha_+ P_T^2 \beta_\psi \sin^2 \theta}{8(\alpha_\psi + 3)}, \\ \frac{d\langle \mu_4 \rangle}{d \cos \theta} &= -\frac{3\alpha_- P_T^2 \beta_\psi \sin^2 \theta}{8(\alpha_\psi + 3)}, \\ \frac{d\langle \mu_5 \rangle}{d \cos \theta} &= \frac{\alpha_- \alpha_+ P_T^2 [(2\alpha_\psi + 1) \cos^2 \theta + \alpha_\psi]}{12(\alpha_\psi + 3)}. \end{aligned} \quad (24)$$

The above moment analysis can be used to intuitively display the polarization information in the $e^+e^- \rightarrow \Lambda\bar{\Lambda}$ process and its transfer in the Λ and $\bar{\Lambda}$ decay. In experiments, the observed variables corresponding to these moments are constructed using kinematic variables detected in the experiment, and the values are taken as the weight factors of each event in the distribution plot. If $P_T = 0$, these moment distributions are trivially flat; if $P_T \neq 0$, they should exhibit a nontrivial distribution described by the Eqs. (24). In order to compare with unweighted events in the experiment, we generate toy Monte-Carlo events using the joint angular distribution formula $\mathcal{W}(\xi)$ for the $e^+e^- \rightarrow \Lambda\bar{\Lambda}$ process, with parameters set to $\Delta\Phi = 0.4$ rad, $\alpha_\psi = 0.69$, $\alpha_- = 0.748$ and $\alpha_+ = -0.757$ [30, 47], and $P_T = 0.5$. The ϕ in Fig. 5 represents the azimuthal angle distribution of Λ , showing the distribution of $d\mathcal{W}(\xi)/d\phi \sim \alpha_\psi P_T^2 \cos(2\phi)$. The $\langle \mu_i \rangle (i = 1, 2, \dots, 5)$ represents the nontrivial moment distributions, providing an intuitive display of the existence of beam transverse polarization. As a reference, the $P_T = 0$ cases are also presented for comparison. It can be observed that they appear as flat distributions with some statistical fluctuations.

B. Statistical significance test

Using the $J/\psi \rightarrow \Lambda\bar{\Lambda}$ decay, the BESIII collaboration has previously studied the decay parameters of Λ and

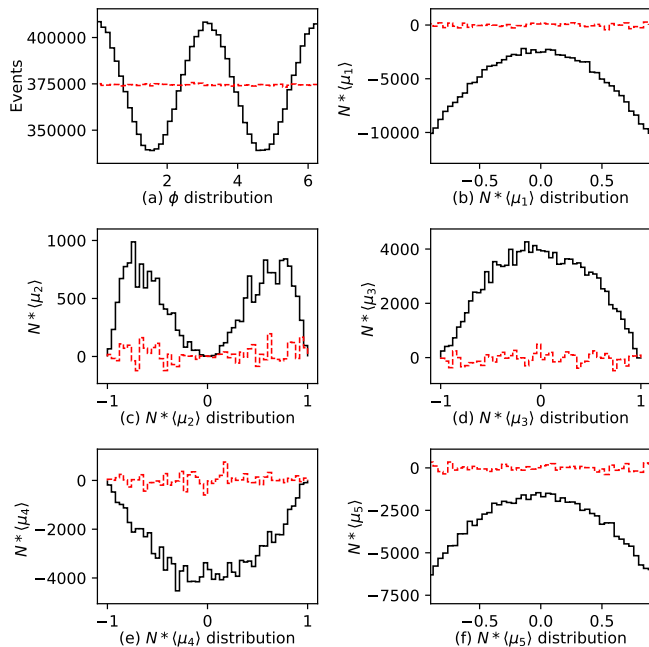


FIG. 5: Various distributions in the $e^+e^- \rightarrow \Lambda\bar{\Lambda}$ process. (a). Λ azimuthal angle distribution, (b-f): moments distributions of $N * \langle \mu_i \rangle$ ($i = 1, 2, \dots, 5$), here N is the number of toy Monte-Carlo events, using $e^+e^- \rightarrow \psi(3686) \rightarrow \Lambda\bar{\Lambda}$ with $\alpha = 0.69$ and $\Delta\Phi = 23^\circ$ radian [30], and dashed histogram is for $P_T = 0$, histogram for $P_T = 0.5$.

$\bar{\Lambda}$, and measured the precise values of α_- and α_+ by fitting the data using the joint angular distribution formula for the 4-body decay. The formula used did not include the contribution of beam transverse polarization. At the J/ψ energy point, due to the depolarization resonance effect, the transverse polarization of the beam becomes very small. However, at the $\psi(3686)$ energy point, the polarization effect of the beam will be more significant. Taking the $\psi(3686) \rightarrow \Lambda\bar{\Lambda}$ decay as an example, we elucidate the role of beam transverse polarization effects in measuring the decay parameters of Λ .

In experiments, the maximum likelihood method is commonly used to measure the decay parameters of Λ , and its statistical error can also be obtained from the fit to the experimental data. For the $\psi(3686) \rightarrow \Lambda\bar{\Lambda}$, $\Lambda \rightarrow p\pi^-$, $\bar{\Lambda} \rightarrow \bar{p}\pi^+$ decay, we define the probability distribution function that describes its joint angular distribution as:

$$\widetilde{\mathcal{W}} = \frac{\mathcal{W}(\theta, \phi, \theta_1, \phi_1, \theta_2, \phi_2)}{\int \mathcal{W}(\dots) d \cos \theta d \cos \theta_1 d \cos \theta_2 d \phi d \phi_1 d \phi_2}. \quad (25)$$

Here, the denominator serves to normalize the probability distribution of the angular distribution. The likelihood function for the observed data sample of N events in the experiment is expressed as:

$$L(\theta, \phi, \theta_1, \phi_1, \theta_2, \phi_2 | \xi) = \prod_{i=1}^N \widetilde{\mathcal{W}}_i, \quad (26)$$

here $\xi = (\alpha_\psi, \Delta\Phi, \alpha_-, \alpha_+, P_T)$ are parameters to be estimated, and the product is computed based on the probability of the i -th event $\widetilde{\mathcal{W}}_i$. According to the maximum likelihood estimation method for parameter estimation, the precision of parameter x_i is expressed as

$$\delta(x_i) = \frac{\sqrt{V(x_i)}}{|x_i|}, \quad (27)$$

where $V(x_i)$ represents the variance of the parameter. We assume that the beam polarization P_T corresponding to the $\psi(3686)$ data sample can be determined through other processes, such as $e^+e^- \rightarrow \mu^+\mu^-$ measurements. The maximum likelihood fit selects four parameters $\alpha_\psi, \Delta\Phi, \alpha_-$ and α_+ , and the error matrix formed by them can be calculated using the following equation:

$$V_{ij}^{-1}(\mathbf{x}) = N \int \frac{1}{\widetilde{\mathcal{W}}} \frac{\partial \widetilde{\mathcal{W}}}{\partial x_i} \frac{\partial \widetilde{\mathcal{W}}}{\partial x_j} d \cos \theta d \cos \theta_1 d \cos \theta_2 d \phi d \phi_1 d \phi_2. \quad (28)$$

Figure 6 shows the measurement sensitivity of estimated $\Delta\Phi$, α_ψ , α_- , and $A_{CP} = \frac{\alpha_- + \alpha_+}{\alpha_- - \alpha_+}$ under different statistical events of $e^+e^- \rightarrow \psi(3686) \rightarrow \Lambda(p\pi^-)\bar{\Lambda}(\bar{p}\pi^+)$. In the absence of transverse beam polarization ($P_T = 0$), the relative error in parameter measurement is maximized for the same data statistical quantity N . As the value of P_T increases from 0.3 to 0.8, it can be observed that the measurement sensitivity of these parameters increases. In other words, the application of transverse beam polarization is advantageous for enhancing the measurement sensitivity of the parameters.

If $\Lambda(\bar{\Lambda}) \rightarrow p\pi^-(p\pi^+)$ decays conserve CP symmetry, their decay parameters satisfy the relation $\alpha_- = -\alpha_+$. If an experiment measures $\alpha_- \neq -\alpha_+$, it implies CP violation in $\Lambda(\bar{\Lambda})$ decays. The significance test for CP asymmetry can be attributed to statistical hypothesis testing as follows. The null hypothesis is that the sum of the Λ and $\bar{\Lambda}$ decay parameters is zero, while the alternative hypothesis is that the sum is not zero. We conduct a test using toy Monte Carlo events generated with parameters $\alpha_\psi = 0.69$, $\Delta\Phi = 23^\circ$ [30], and $\alpha_- = 0.748$ and $\alpha_+ = -0.757$ [30, 47] for different transverse polarizations $P_T = 0, 0.5$ and 0.8 . The significance is calculated as $\sqrt{-2 \ln L_0 - (-2 \ln L_1)}$, where L_0 and L_1 are the log-likelihood values for the null and alternative hypotheses, respectively. Using the likelihood function defined in Eq.(26), L_0 is calculated with $\alpha_- = -\alpha_+ = 0.7525$, while L_1 is calculated with $\alpha_- = 0.748$ and $\alpha_+ = -0.757$ under different P_T assumptions. The significance is shown in Fig. 7 as a function of the number of observed events. It can be observed that the significance benefits from the non-zero transverse polarization of the e^+e^- beams.

IV. SUMMARY AND PERSPECTIVES

In summary, high-energy lepton beams naturally acquire transverse polarization in a storage ring through

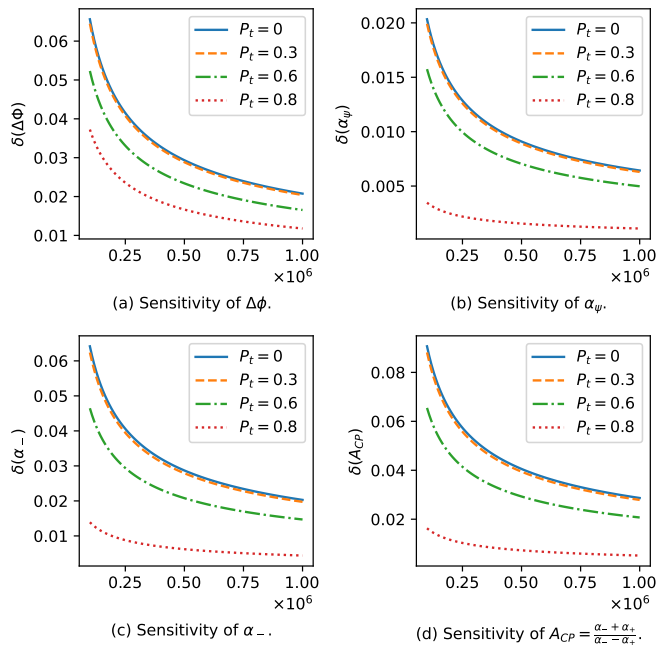


FIG. 6: Sensitivity of $\Delta\Phi$, α_ψ , α_- and $A_{CP} = (\alpha_- + \alpha_+)/(\alpha_- - \alpha_+)$ in terms of data size N , using $e^+e^- \rightarrow \psi(3686) \rightarrow \Lambda\bar{\Lambda}$ with $\alpha_\psi = 0.69$, $\Delta\Phi = 23^\circ$ [30], and $\alpha_- = 0.748$ and $\alpha_+ = -0.757$ [30, 47].

the mechanism of self-polarization, known as the Sokolov-Ternov effect. We investigate the impact of transversely polarized beams on the observables of hyperon production and sequential decay at an electron-positron collider, utilizing helicity amplitude analysis. It is shown that the transverse polarization of the beams introduces a new azimuthal modulation of the events in terms of the azimuthal angle of hyperons in the laboratory frame. Through moments analysis and maximum likelihood estimation, we characterize the statistical uncertainties that transversely polarized beams may impose on constraining CP violation parameters. As demonstrated in this paper, the sensitivity to measure the hyperon decay parameter and CP violation can be enhanced by employing transversely polarized electron and positron beams. In our study, we consider $e^+e^- \rightarrow \gamma^*/\psi \rightarrow \Lambda(p\pi^-)\bar{\Lambda}(\bar{p}\pi^+)$ and $\Xi^-(\Lambda\pi^-)\bar{\Xi}^+(\bar{\Lambda}\pi^+)$ as examples. However, the sensitivity remains largely unchanged if the transverse polarization of beam is small, e.g. in the case of J/ψ decay at BESIII. Therefore, previous measurements of J/ψ decays are not affected even if the transverse polarization of beams is considered. On the other hand, at the energies of big po-

larization degree, e.g. $\psi(3686)$, we recommend the inclusion of this effect in future data analyses at e^+e^- circular colliders, and suggest extending the formalism in this paper to other processes such as $e^+e^- \rightarrow \Sigma^+(p\pi^0)\bar{\Sigma}^-(\bar{p}\pi^0)$, $\Lambda_c^+(\Lambda\pi^+)\bar{\Lambda}_c^-(\bar{\Lambda}\pi^-)$ and $\Omega^-(\Lambda K^-)\bar{\Omega}^+(\bar{\Lambda}K^+)$ [48, 49] for comprehensive investigations. This effect on other observables, such as higher-order quantum electrodynamic

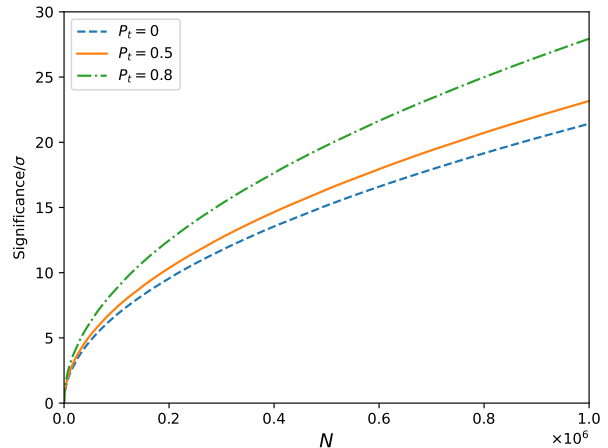


FIG. 7: Significance test for CP asymmetry in $\Lambda(\bar{\Lambda}) \rightarrow p\pi^-(p\pi^+)$ decays as a function of the number of observed events N , using toy Monte Carlo events for $e^+e^- \rightarrow \psi(3686) \rightarrow \Lambda\bar{\Lambda}$ generated with parameters $\alpha_\psi = 0.69$, $\Delta\Phi = 23^\circ$ [30], and $\alpha_- = 0.748$ and $\alpha_+ = -0.757$ [30, 47] for different transverse polarizations $P_t = 0, 0.5$ and 0.8 .

processes, hyperon weak radiative decays (e.g., [50, 51]), and hadronic vacuum polarization, is a topic of future interest as well.

Acknowledgments

We are grateful to Jianping Dai, Zhe Duan, Boxing Gou, Andrzej Kupsc, Xiongfei Wang, Jujun Xie, and Xiaorong Zhou for useful discussions. This work is supported by the National Key R&D Program of China under Grant No. 2023YFA1606703, the National Natural Science Foundation of China (Grants Nos.12075289, 12175244, U2032109) and the Strategic Priority Research Program of Chinese Academy of Sciences (Grant No. XDB34030301).

[1] B. Ananthanarayan and S. D. Rindani, Phys. Rev. D **70**, 036005 (2004), hep-ph/0309260.
 [2] G. Moortgat-Pick et al., Phys. Rept. **460**, 131 (2008), hep-ph/0507011.

[3] X.-K. Wen, B. Yan, Z. Yu, and C. P. Yuan, Phys. Rev. Lett. **131**, 241801 (2023), 2307.05236.
 [4] S. H. Chen et al., JINST **17**, P08005 (2022).
 [5] A. A. Sokolov and I. M. Ternov, Dokl. Akad. Nauk SSSR

- 153**, 1052 (1963).
- [6] V. N. Baier and V. S. Fadin, *Sov. Phys. Dokl.* **10**, 204 (1965).
- [7] J. D. Jackson, *Rev. Mod. Phys.* **48**, 417 (1976).
- [8] B. W. Montague, *Phys. Rept.* **113**, 1 (1984).
- [9] L. M. Kurdadze, S. I. Serebnyakov, V. A. Sidorov, A. N. Skrinsky, G. M. Tumaikin, and Y. M. Shatunov, *Sov. Phys. JETP* **44**, 1063 (1976).
- [10] J. G. Learned, L. K. Resvanis, and C. M. Spencer, *Phys. Rev. Lett.* **35**, 1688 (1975).
- [11] L. Knudsen, J. P. Koutchouk, M. Placidi, R. Schmidt, M. Crozon, J. Badier, A. Blondel, and B. Dehning, *Phys. Lett. B* **270**, 97 (1991).
- [12] S. Nikitin, *Int. J. Mod. Phys. A* **34**, 1940004 (2019).
- [13] A. Blondel et al. (2019), 1909.12245.
- [14] D. M. Asner et al. (US Belle II Group, Belle II/SuperKEKB e- Polarization Upgrade Working Group), in *Snowmass 2021* (2022), 2205.12847.
- [15] M. Achasov et al., *Front. Phys. (Beijing)* **19**, 14701 (2024), 2303.15790.
- [16] H. Czyz, A. Grzelinska, and J. H. Kuhn, *Phys. Rev. D* **75**, 074026 (2007), hep-ph/0702122.
- [17] H. Chen and R.-G. Ping, *Phys. Rev. D* **76**, 036005 (2007).
- [18] G. Fäldt and A. Kupsc, *Phys. Lett. B* **772**, 16 (2017), 1702.07288.
- [19] T. D. Lee and C.-N. Yang, *Phys. Rev.* **108**, 1645 (1957).
- [20] J. F. Donoghue and S. Pakvasa, *Phys. Rev. Lett.* **55**, 162 (1985).
- [21] J. F. Donoghue, X.-G. He, and S. Pakvasa, *Phys. Rev. D* **34**, 833 (1986).
- [22] N. Salone, P. Adlarson, V. Batzskaya, A. Kupsc, S. Leupold, and J. Tandean, *Phys. Rev. D* **105**, 116022 (2022), 2203.03035.
- [23] S. Zeng, Y. Xu, X. R. Zhou, J. J. Qin, and B. Zheng, *Chin. Phys. C* **47**, 113001 (2023), 2306.15602.
- [24] A. Z. Dubnickova, S. Dubnicka, and M. P. Rekalov, *Nuovo Cim. A* **109**, 241 (1996).
- [25] S. J. Brodsky, C. E. Carlson, J. R. Hiller, and D. S. Hwang, *Phys. Rev. D* **69**, 054022 (2004), hep-ph/0310277.
- [26] E. Tomasi-Gustafsson, F. Lacroix, C. Duterte, and G. I. Gakh, *Eur. Phys. J. A* **24**, 419 (2005), nucl-th/0503001.
- [27] Y.-S. Tsai, *Phys. Rev. D* **12**, 3533 (1975).
- [28] F. Bletzacker and H. T. Nieh, *Phys. Rev. D* **14**, 1251 (1976).
- [29] K.-i. Hikasa, *Phys. Rev. D* **33**, 3203 (1986).
- [30] M. Ablikim et al. (BESIII), *JHEP* **10**, 081 (2023), [Erratum: *JHEP* 12, 080 (2023)], 2303.00271.
- [31] M. Ablikim et al. (BESIII), *Phys. Rev. Lett.* **125**, 052004 (2020), 2004.07701.
- [32] M. Ablikim et al. (BESIII), *Phys. Rev. D* **105**, L011101 (2022), 2111.11742.
- [33] M. Ablikim et al. (BESIII), *Phys. Rev. D* **106**, L091101 (2022), 2206.10900.
- [34] H. Liu, J. Zhang, and X. Wang, *Symmetry* **15**, 214 (2023).
- [35] M. Ablikim et al. (BESIII), *Phys. Rev. D* **108**, L011101 (2023), 2302.09767.
- [36] M. Ablikim et al. (BESIII), *Phys. Rev. D* **100**, 051101 (2019), 1907.13041.
- [37] M. Ablikim et al. (BESIII), *Phys. Rev. Lett.* **126**, 092002 (2021), 2007.03679.
- [38] J.-P. Dai, X. Cao, and H. Lenske, *Phys. Lett. B* **846**, 138192 (2023), 2304.04913.
- [39] E. Perotti, G. Fäldt, A. Kupsc, S. Leupold, and J. J. Song, *Phys. Rev. D* **99**, 056008 (2019), 1809.04038.
- [40] J. Z. Bai et al. (BES), *Phys. Lett. B* **355**, 374 (1995), [Erratum: *Phys.Lett.B* 363, 267 (1995)].
- [41] M. Ablikim et al. (BESIII), *Phys. Lett. B* **791**, 375 (2019), 1808.02166.
- [42] V. V. Anashin et al., *Phys. Lett. B* **781**, 174 (2018), 1801.10362.
- [43] P.-C. Hong, R.-G. Ping, T. Luo, X.-R. Zhou, and H. Li, *Chin. Phys. C* **47**, 093103 (2023), 2306.08517.
- [44] H. Chen and R.-G. Ping, *Phys. Rev. D* **99**, 114027 (2019).
- [45] G. Fäldt, *Phys. Rev. D* **97**, 053002 (2018), 1709.01803.
- [46] M. Ablikim et al. (BESIII), *Phys. Rev. D* **100**, 072004 (2019), 1905.04707.
- [47] M. Ablikim et al. (BESIII), *Nature Phys.* **15**, 631 (2019), 1808.08917.
- [48] Z. Zhang and J. J. Song, *Chin. Phys. C* **47**, 093101 (2023), 2303.02629.
- [49] Z. Zhang, J. J. Song, and Y.-j. Zhou, *Phys. Rev. D* **109**, 036005 (2024), 2312.04363.
- [50] R.-X. Shi, S.-Y. Li, J.-X. Lu, and L.-S. Geng, *Sci. Bull.* **67**, 2298 (2022), 2206.11773.
- [51] Z.-P. Xing, Y. J. Shi, J. Sun, and Z.-X. Zhao (2023), 2312.17568.